Environmental Influences on Mn-Oxide Catalyzed Arsenic Oxidation

S.J. Parikh[1], B.J. Lafferty[2], and D.L. Sparks[2]

[1]Department of Land, Air and Water Resources, University of California, Davis; [2]Department of Plant and Soil Sciences, University of Delaware

Research Objective

The oxidation of arsenite (As^{III}) via Mn-oxides is an important process for arsenic cycling and *in situ* remediation of As-contaminated waters. Under natural conditions the presence of additional mineral surfaces, bacteria, biopolymers, organic matter, and ions in solution can serve to block Mn-oxide reaction sites and retard or inhibit As^{III} oxidation. ***Therefore, the primary objective of this research is to examine the rapid oxidation of As^{III} via Mn-oxides in the presence of competing ions, mineral surfaces, and bacteria/biopolymers coatings.***

Arsenic in the Critical Zone

What is the Critical Zone?

The Critical Zone (Fig. 1) is the heterogeneous, near surface environment in which interactions involving rock, soil, water, air, and living organisms regulate the natural habitat and determine the availability of life-sustaining resources.

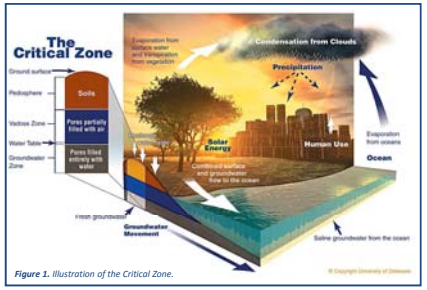

Figure 1. *Illustration of the Critical Zone.*

Why Arsenic?

Arsenic (As) is a toxic element that can have detrimental effects on human health. The primary source of As in the environment is the weathering of As-bearing rocks (Fig. 2a).

Exposure to As is commonly through ingestion of As contaminated drinking water. Arsenic poisoning can cause many ailments including cancer. Figure 2b shows excessive pigmentation on the hands and feet of two Bangladeshi men, an early symptom of As poisoning.

Figure 2. *(a) Naturally occurring As concentrations (grey) in rock and (b) As poisoning symptoms: excess pigmentation on hands and feet.*

Sources of Arsenic in the Critical Zone

Arsenic contamination from natural and anthropogenic sources include:

- historical use of pesticides/fertilizers
- coal combustion
- land application of sewage sludge
- industrial waste
- land application of animal waste
- rocks and minerals

Arsenic Transformations Influence Mobility and Toxicity

The mechanisms and initial reaction rates of As transformations via microorganisms and mineral surfaces are still largely unknown. These transformations influence As toxicity, mobility, and bioavailability.

Rapid-Scan FTIR Analysis of As^{III} Oxidation

Rapid-scan attenuated total reflectance (ATR) Fourier transform infrared (FTIR) was used to investigate the initial oxidation of As^{III} via hydrous Mn-oxide (HMO). Rapid-scan ATR-FTIR collect rapid data (2 to 12 sec) for real time, *in situ*, non-destructive monitoring of As redox transformations at the solid/liquid interface.

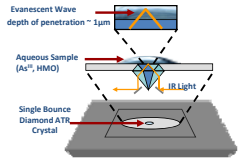

Figure 3. *Schematic illustration of rapid-scan ATR-FTIR spectroscopy.*

Biological Transformation of Arsenic

Oxidation of As^{III} to As^{V} in the Critical Zone results in a less toxic and less mobile species of As. Over 30 strains of bacteria have been isolated which can oxidize As; either as a means of detoxification or as a means to gain energy. These bacteria play an important role in As biogeocycling. The As-oxidizing bacteria used in the study include *Variovorax paradoxus, Agrobacterium tumefaciens , Alcaligenes faecalis* , and *Pseudomonas fluorescens* .

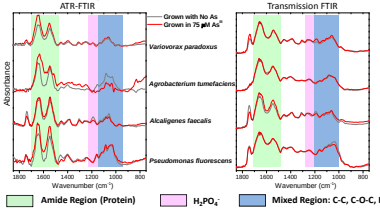

Figure 4. *FTIR spectra of four As-oxidizing bacteria collected before and after As^{III} oxidation using a) ATR and b) transmission sampling techniques.*

·ATR spectra are biased to surface moieties; transmission spectra represent the bulk sample.

·Differences between ATR and transmission spectra after As^{III} oxidation likely indicate a change in conformation and/or content of surface proteins (e.g., enzymes) involved in As^{III} oxidation (Fig. 4).

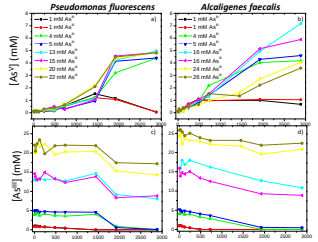

Figure 5. *Kinetic plots of As^{III} oxidation by P. fluorescens [a) As^{V} solution concentration, c) As^{III} solution concentrations] and A. faecalis [b) As^{V} solution concentration and d) As^{III} solution concentration] for initial As^{III} concentrations ranging from 1 to 26 mM.*

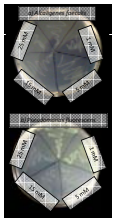

Figure 6. *Streak plates of a) A. faecalis and b) P. fluorescens after 48 h of growth in the presence of 0, 1, 5, 15, and 25 mM As^{III}.*

·Bacteria completely oxidize 1 mmol kg^{-1} As^{III} in approximately 24 h (Fig. 5).

·Bacteria oxidize a maximum As^{III} concentration of about 5 mmol kg^{-1} within 48 h, with the highest rate of oxidation occurring after the first 24 h of reaction (Fig 5).

·The growth of bacteria colonies or R2A agar plates after 48 h demonstrates the levels of As used are non-lethal (Fig. 6).

Mineralogical Transformation of Arsenic

Soil minerals (Mn and Fe-oxides) can play an important role in oxidation of As^{III} in the Critical Zone. Common As oxidation pathways in soils and the general reaction for As^{III} oxidation by Mn-oxides are shown in Figure 7.

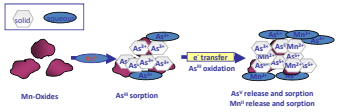

Figure 7. *Illustration for As oxidation on Mn-oxide surfaces.*

Arsenic Sorption to Hydrous Mn-Oxide

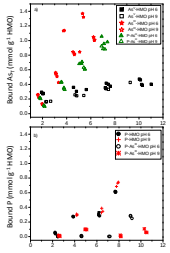

Figure 8. *Sorption isotherms from batch experiments conducted at pH 6 (solid symbols) and 9 (open symbols) in 5 mM NaCl for a) As sorption to HMO when added as As^{V} and As^{III} (including oxidation) in the presence and absence of phosphate (P); b) phosphate sorption to HMO in the presence and absence of As^{III}.*

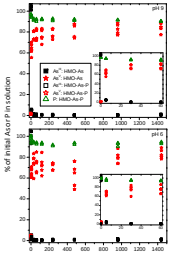

Figure 9. *Kinetic plots of batch experiments showing the percent of initial As (5 mM As^{III}), as solution As^{III} and As^{V}, and phosphate in solution during reaction with HMO at a) pH 9 and b) pH 6 in 5 mM NaCl. Solid symbols correspond to experiments where HMO was reacted with As^{III} and open symbols correspond to experiments where As^{III} and phosphate were simultaneously reacted with HMO.*

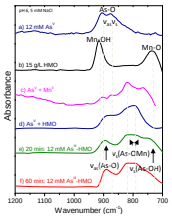

Figure 10. *ATR-FTIR spectra (diamond IRE) of a) 12 mM As^{V} standard, b) 15 g L^{-1} HMO standard, c) As^{V} reacted with Mn^{II} ($MnCl_2$), d) As^{V} reacted with HMO, and 12 mM As^{III} reacted with HMO for e) 20 and f) 60 min.*

·Rapid oxidation of As^{III} upon reaction with hydrous Mn-oxide (HMO) – a relatively amorphous mineral similar to birnessite.

·Increased retention of As to HMO when As^{III} is added instead of As^{V} (Fig. 8).

·Competition between As^{V} and phosphate leads to decreased retention of both anions (Fig. 8).

·Concentration of As^{III} (initial 5 mmol kg^{-1}) in solution rapidly drops to near zero; As^{V} concentrations do not level off for up to 960 min (Fig. 9).

·Rapid oxidation of As^{III} upon binding to Mn^{IV} accounts for most of the reaction; however, binding of Mn^{III} to HMO followed by As^{III} sorption to Mn^{III}-HMO may be lead to much slower As^{III} oxidation and account for As^{V} release to solution between 30 and 960 min (Fig. 9).

·ATR-FTIR spectra of standards and As^{III} reacted with HMO indicate that As^{V} primarily binds to HMO through Mn^{IV} sites, with some binding via Mn^{II} (Fig. 10).

Rapid As^{III} Oxidation via HMO

- Rapid-scan ATR-FTIR data reveal rapid initial As^{III} oxidation regardless of pH or HMO concentration (Fig. 11, 12), with most of the initial reaction is complete within the first 2 min. As oxidation is inhibited due to passivation of the mineral surface through reaction products binding and blocking Mn^{IV} sites.

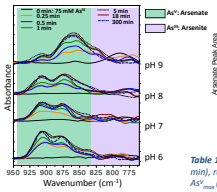

Figure 11. *ATR-FTIR spectra for HMO reacted with As^{III} (pH 6, 7, 8, 9). Within 1 min As^{V} peaks (860, 873, 906 cm^{-1}) are observed; minimal subsequent changes are observed.*

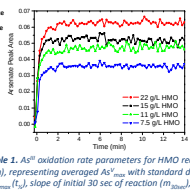

Figure 12. *Rapid-scan ATR-FTIR plots of As^{V} IR peak area as a function of reaction time for 25 mM As^{III} reacted with varying concentrations of HMO suspensions at pH 6 in 5 mmol kg^{-1} NaCl.*

Table 1. *As^{III} oxidation rate parameters for HMO reaction with 25 mM As^{III} (15 min), representing averaged As^{V}_{max} with standard deviation, time to reach half As^{V}_{max} ($t_{1/2}$), slope of initial 30 sec of reaction (m_{30sec}), and corresponding R^2*

	22 g kg^{-1} HMO	15 g kg^{-1} HMO	11 g kg^{-1} HMO	7.5 g kg^{-1} HMO
$[As^{V}_{max}]$	17.9 (4.81)	14.7 (3.91)	13.2 (3.86)	9.80 (2.95)
$t_{1/2}$ (min)	0.28	0.22	0.21	0.28
$R^2_{t1/2}$	0.97	0.94	0.91	0.93
m_{30s}	0.10	0.10	0.09	0.06
R^2_{30s}	1.00	0.93	0.80	0.85

Environmental Influences on As^{III} Oxidation

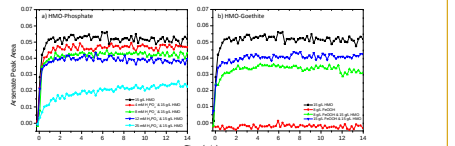

Figure 13. *Rapid-scan ATR-FTIR plots of As^{V} IR peak area as a function of reaction time for 25 mM As^{III} (pH 6, 5 mM NaCl) reacted with varying concentrations of a) phosphate (P) and b) α-FeOOH.*

Table 2. *As^{III} oxidation rate parameters for HMO reaction with 25 mM As^{III} (15 min) and varying concentration of phosphate (P).*

	15 g L^{-1} HMO				
	0 mM P	4 mM P	8 mM P	12 mM P	25 mM P
$[As^{V}_{max}]$	14.7 (3.91)	13.1 (3.56)	11.8 (3.53)	10.8 (3.00)	5.40 (2.08)
$t_{1/2}$ (min)	0.22	0.25	0.30	0.19	1.04
$R^2_{t1/2}$	0.94	0.96	0.94	0.94	0.92
m_{30s}	0.10	0.08	0.09	0.08	0.02
R^2_{30s}	0.93	0.97	0.86	0.94	1.00

Table 3. *As^{III} oxidation rate parameters for HMO reaction with 25 mM As^{III} (15 min) and varying concentration of α-FeOOH.*

	15 g L^{-1} HMO		
	0 g kg^{-1} α-FeOOH	8 g kg^{-1} α-FeOOH	15 g kg^{-1} α-FeOOH
$[As^{V}_{max}]$	14.7 (3.91)	9.17 (2.93)	11.4 (2.99)
$t_{1/2}$ (min)	0.22	0.22	0.16
$R^2_{t1/2}$	0.94	0.85	0.91
m_{30s}	0.10	0.06	0.06
R^2_{30s}	0.93	0.46	0.98

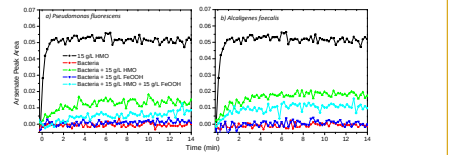

Figure 14. *Rapid-scan ATR-FTIR plots of As^{V} IR peak area as a function of reaction time for 25 mM As^{III} (pH 6, 5 mM NaCl) reacted with a) P. fluorescens and b) A. faecalis suspensions (10 times steady state) with and without HMO and α-FeOOH.*

·The addition of phosphate and α-FeOOH serves to reduce the amount of As^{V} produced; the oxidation rate is generally not affected (Fig 13, Table 2 and 3).

·Binding of phosphate (similar chemical structure to As^{V}) to Mn-oxides blocks As^{III} reaction sites and hinders oxidation (Fig 8 and 12).

·The addition of α-FeOOH leads to competition for As^{III}, and therefore reduced As^{III} binding and subsequent oxidation.

·At high α-FeOOH (15 g/L) concentrations As^{V} released from HMO during oxidation is bound to α-FeOOH instead of HMO; surface passivation is reduced and there is increased detection of As^{V} (Fig. 13b).

·The presence of bacteria on HMO hinders As^{V} production (Fig. 14) much more than reaction with phosphate of α-FeOOH and reaction rates are significantly reduced, based on $t_{1/2}$ and m_{30s} values (Table 4).

·Bacterial adhesion to mineral surfaces results in a coating which blocks access to Mn^{IV} and therefore reduces As^{V}_{max}.

Table 4. *As^{III} oxidation rate parameters for reaction of HMO with 25 mM As^{III} (5 mM NaCl, pH 6, 15 min reaction) and bacteria (P. fluorescens an A. faecalis) and α-FeOOH*

	15 g L^{-1} HMO				
	No Bacteria	P. fluorescens	A. faecalis	P. fluorescens + 15 g kg^{-1} α-FeOOH	A. faecalis + 15 g kg^{-1} α-FeOOH
$[As^{V}_{max}]$	14.7 (3.91)	3.05 (1.23)	4.41 (1.66)	0.79 (0.84)	2.14* (1.05)
$t_{1/2}$ (min)	0.22	1.01	0.95	2.81	0.98
$R^2_{t1/2}$	0.94	0.73	0.88	0.68	0.64
m_{30s}	0.10	0.01	0.01	0.01	0.01
R^2_{30s}	0.93	0.94	0.79	0.79	1.00

Summary

·Competing factors generally reduce, or inhibit, the initial As^{III} oxidation reaction and their presence should be considered when trying to determine the fate of As in natural settings.

·Additional work is needed to look at long term reaction rates for As-oxidizing bacteria bound to Mn-oxide surfaces; increased time may permit abiotic and biotic reactions to work simultaneously.

·The potential for Fe-oxides to bind reaction products should be further explored. Fe-oxides are ubiquitous in soils and subsurface environments and their presence at levels greater then Mn-oxides may serve to greatly reduce surface passivation and permit greater As oxidation and subsequent sequestration.

Acknowledgements: